View Online / Journal Homepage / Table of Contents for this issue
Dynamic Article Links

Soft Matter

Cite this: *Soft Matter*, 2012, **8**, 6740

www.rsc.org/softmatter

PAPER

An underwater pH-responsive superoleophobic surface with reversibly switchable oil-adhesion†

Qunfeng Cheng,‡[a] Mingzhu Li,‡[b] Fu Yang,‡[c] Mingjie Liu,[b] Lin Li,[c] Shutao Wang*[b] and Lei Jiang[ab]

Received 23rd February 2012, Accepted 19th April 2012
DOI: 10.1039/c2sm25421b

An underwater pH-responsive superoleophobic surface successfully demonstrated a reversible switch of oil-adhesion on a nanostructured poly(acrylic acid) (PAA) surface by changing the environmental pH values. At low pH, intramolecular hydrogen bonding of PAA is formed, and results in high oil-adhesion. As for high pH, the oil droplets can easily roll off due to the intermolecular hydrogen bonding between PAA and surrounding water.

Underwater superoleophobic interfacial materials, mimicking fish scales[1] and the lower side of lotus leaves,[2] as novel fluoride-free interfacial materials, show some fantastic practical applications,[3] *i.e.* novel "water-repelling type" oil/water separation systems.[4] In particular, the control of oil-adhesion on underwater superoleophobic surfacees is of importance and demanded for bio-adhesion,[5] micropatterning,[6] and smart microfluidic gates.[7] Several efforts[5,8,9] have been devoted to explore underwater superoleophobic surfaces with controllable oil-adhesion by designing special micro/nanoscale hierarchical structures, such as robust coatings by mimicking the low adhesive surface of soil animal body, for example, dung beetle, ground beetle,[8] the poly (*N*-isopropylacrylamide) coated nanowire arrays (SiNWA) surface,[5] colloidal crystals films assembled from nonspherical latex particles,[9] and thermally-responsive surfaces.[10] However, to develop an environmentally stimuli-responsive surface with switchable oil-adhesion remains a great challenge.

In this article, we report a smart underwater superoleophobic surface made from nanostructured poly(acrylic acid) (PAA) with reversible pH-switchable oil-adhesion. The oil-adhesion properties on the as-prepared surface can be reversibly tuned by altering environmental pH values. This smart switch originates from the transition between intramolecular and intermolecular hydrogen bonding of PAA. We believe that these surfaces, with switchable oil-adhesion, will bring many potential applications in various biological and industrial fields.

Smart materials have been widely utilized to tune surface wettability because their molecular conformation can be responsive to external stimuli,[11] such as electrical potential,[12] enthalpy,[13] temperature,[14] pH,[15] *etc.* Herein, we prepared a smart nanostructured film by grafting the pH-responsive polymer PAA[16] onto a glass substrate (PAA-G) through a plasma polymerization process (Fig. 1). As a facile method of surface modification, plasma polymerization is able to prepare thin films of polymer on a variety of substrates producing high adhesion and high resistance to chemical and physical treatments.[17] After plasma polymerization, the linear PAA chains were grafted on the glass surface and the thickness of PAA, calculated by atomic force microscopy (AFM), was about 64.5 ± 9.2 nm (see ESI,† Fig. S1) The surface of the PAA-G in solution with a pH value of 2.4 exhibits rough morphology as shown by the underwater AFM image (Fig. 1b). The surface morphology becomes smooth when immersing PAA-G into a solution with a pH value of 8.0 (Fig. 1c). The blue dash rectangle in Fig. 1b and 1c is used to mark the same location in the *in situ* processing of underwater AFM testing. The blue dash rectangle mark proves the *in situ* transition of surface morphology on PAA-G when the pH value of solution is greater than the pK_a of PAA. The surface roughness decreases from about 5 nm to 1 nm, when the pH value changes from 2.4 to 8.0. In air, the original glass substrate is hydrophilic, with a water contact angle (CA) of 34.3 ± 3.0° (see ESI,† Fig. S2a). After plasma-induced grafting of PAA, the PAA-G shows superhydrophilicity with a CA of 9.0 ± 1.5° (see ESI,† Fig. S2b). This change of surface wettability indicates a change of chemical composition and surface roughness.[18] After plasma etching, a little part of glass is etched out which results in a rougher surface morphology. The underwater AFM image of plasma treated glass shows that the roughness increases to about 2 nm from about 0 nm (see ESI,† Fig. S3). The carboxylic pendant groups of PAA accept protons at a pH value lower its pK_a of 4.7[19] (insert in Fig. 1a), release them with an increase of pH value and transform into polyelectrolytes due to electrostatic repulsion forces of the molecular chains.[20] The conformation of

[a]*Key Laboratory of Bio-inspired Smart Interfacial Science and Technology of Ministry of Education, School of Chemistry and Environment, BeiHang University, Beijing 100191, China*
[b]*Beijing National Laboratory for Molecular Sciences (BNLMS), Key Laboratory of Organic Solids, Laboratory of New Materials, Institute of Chemistry, Chinese Academy of Sciences, Beijing 100190, China. Fax: (+86) 10-8262-1396; E-mail: stwang@iccas.ac.cn; (+86) 10-8262-7566*
[c]*College of Chemistry, Beijing Normal University, Beijing 100875, China*
† Electronic Supplementary Information (ESI) available: See DOI: 10.1039/c2sm25421b/
‡ These authors contributed equally to this work.

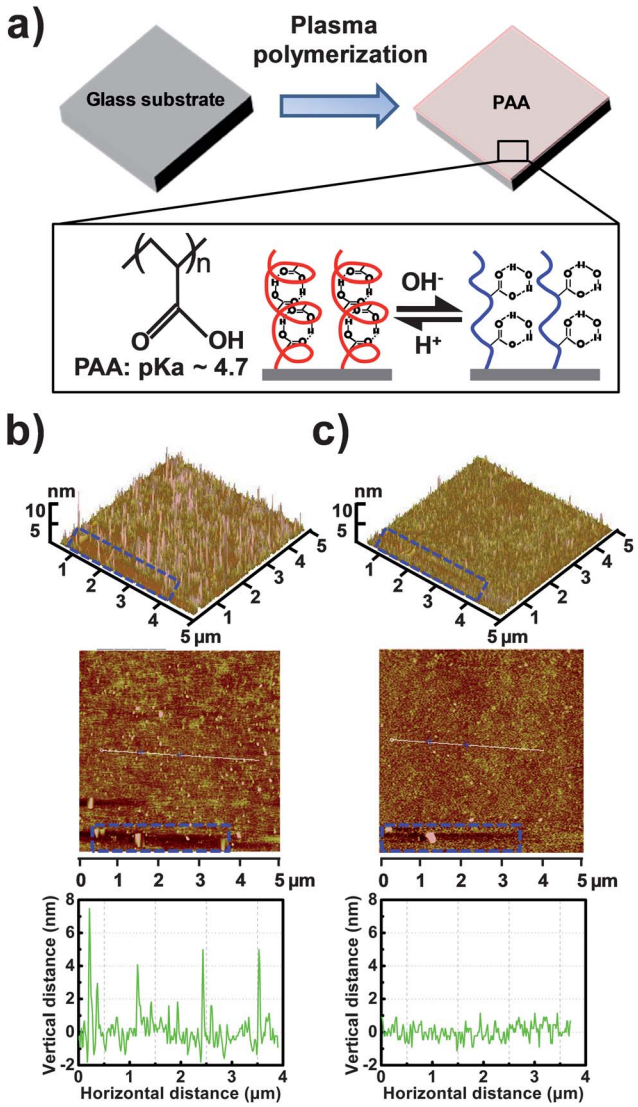

Fig. 1 The pH-responsive PAA surface with switchable underwater oil-adhesion, grafted by a plasma polymerization. (a) The PAA was grafted onto glass substrate (PAA-G) by the plasma polymerization process. The pH-responsive schematics of the conformation switch of PAA: the intramolecular hydrogen bonds form among the carboxylic acid groups on the PAA chains when the pH value is below pK_a, and the intermolecular hydrogen bonds form between PAA chains and water molecules when the pH is above the pK_a. (b) Underwater atomic force microscopy (AFM) image of PAA-G in the solution with a pH value of 2.4 shows rough morphology with a roughness of about 5 nm. (c) When PAA-G is in solution with pH value of 8.0, the *in situ* AFM image becomes smooth with a roughness of about 1 nm. The blue dash rectangle in Fig. 1b and 1c shows the mark in the *in situ* processing of underwater AFM testing.

PAA changes from coiled at low pH to stretched at high pH,[21] schematically outlined in Fig. 1a (lower insert). At low pH, the formation of intramolecular hydrogen bonds prevail in PAA films, while at high pH intermolecular hydrogen bonds were formed between surrounding water molecules and PAA instead of intramolecular hydrogen bonds.

We tested the pH response of the PAA-G surface on underwater oil-adhesion properties. Due to the morphology transition of PAA at pH values above the pK_a of PAA, solutions with pH values of 1.0, 2.4, 4.0, 4.6, 5.0, 8.0 and 12.0 were chosen for different environmental solutions. A 2 μL droplet of 1,2-dichloroethane with surface tension of 24.15 mNm^{-1} was chosen as the oil probe to characterize the pH-responsive switchable adhesion on the PAA-G surface. The adhesive forces between the oil droplet and PAA-G surface were quantitatively measured by a high sensitivity microelectromechanical balance system during a whole approaching, contacting and leaving process. Take the solution with pH value of 1.0 as an example; force–distance curves recorded before and after the oil droplet contacts with the PAA-G is shown in Fig. 2. Process 1: the PAA-G surface approaches the oil droplet; Process 2: the PAA-G surface leaves the oil droplet after contact; Process 3: the PAA-G surface breaks away from the oil droplet. The inset photographs of the shapes of the oil droplets were taken at the corresponding stages during the measuring process (see more details in the ESI,† Fig. S4).

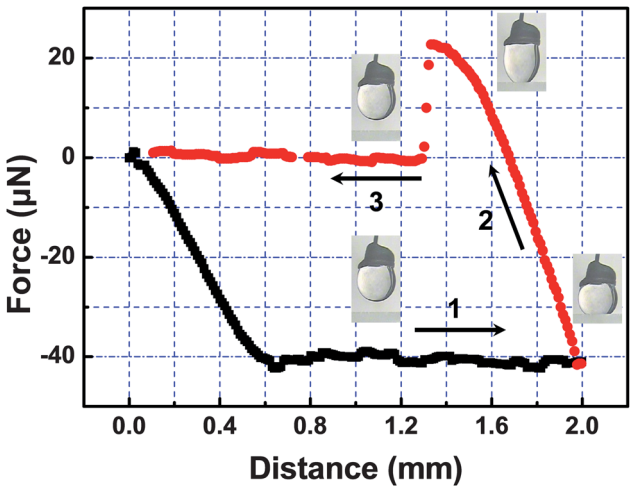

Fig. 2 Force–distance curves recorded before and after PAA-G contacts with the oil droplet in solution with pH value of 1.0. Process 1: PAA-G surface approaches the oil droplet; Process 2: PAA-G surface leaves the oil droplet after contact; Process 3: PAA-G surface breaks away from the oil droplet. The inset photographs of the shapes of the oil droplets were taken at the corresponding stages during the measuring process.

The underwater oil-adhesion on the surface of PAA-G changes with pH values increasing from 1.0 to 12.0, as shown in Fig. 3. Because the pK_a of PAA is around 4.7, the oil-adhesion dramatically decreases with pH values increasing from 4.6 to 5.0. When the pH value is below 4.7, the PAA-G exhibits high adhesion to the oil droplet, and always draws oil droplets with a certain distortion. However, there is no oil residuum on the PAA-G when the oil droplet leaves. At a pH value of 1.0, the recorded adhesive force reaches up to 21.6 ± 5.0 μN. With increasing the pH values from 1.0 to 4.6, the adhesive force decreases to 15.0 ± 2.9 μN. Further increasing pH values above the pK_a of PAA, the oil-adhesion dramatically decrease to 2.0 ± 0.6 μN with a pH value of 5.0, 1.5 ± 0.4 μN with a pH value of 8.0 and zero with a pH value of 12.0. In addition, we carried out the underwater *in situ* transition experiment from low to high adhesion between the PAA-G and oil droplet. The PAA-G was firstly immersed into 0.01 mol l^{-1} sodium hydroxide (NaOH, pH = 12.0) solution and an oil droplet was dropped onto its surface keeping a spherical shape. Then 0.1 mol l^{-1} hydrochloric acid (HCl, pH = 1.0) was quickly added, resulting in the pH value

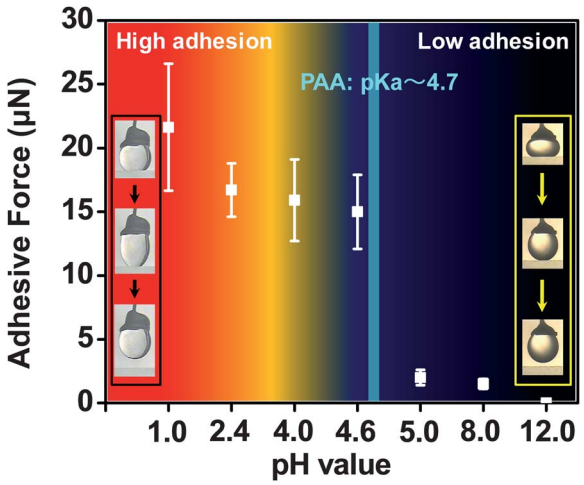

Fig. 3 The influence of pH values on the adhesive force between the as-prepared PAA-G surface and an oil droplet of 1,2-dichloroethane. With the pH values increasing from 1.0 to 12.0, the adhesive force dramatically decreases from 21.6 ± 5.0 μN at a pH value of 1.0 to zero at a pH value of 12.0. The dramatic decrease happens at a pH value of 5.0 above the pK_a of PAA. The inset photographs are the three-step measuring process, from up to down: the oil droplet is contacting the surface of PAA-G, the oil droplet is leaving the surface and the oil droplet has left the surface.

quickly switching from 12.0 to 1.0. The adhesive force switches from low to high in around one second, as shown in Fig. 4a and the *in situ* changing process is shown in the ESI,† Movie S1. The PAA-G was kept in solution with pH values of 1.0 and 12 for 72 h. The pH-responsive behavior still worked, indicating that the good durability of PAA. Therefore, the adhesive force can be easily tuned between high and low by adjusting the environmental pH values. We also performed a similar experiment on the original glass substrate and never found the oil-adhesion transition with increasing pH values. The oil contact angle (OCA) on the original glass substrate shows a slight increase from 132.3 ± 3.8° to 135.9 ± 1.9° with pH values increasing from 2.4 to 8.0 (see ESI,† Fig. S5).

On the other hand, to further verify the pH-responsive switchable oil-adhesion on the PAA-G, other oils with different surface tensions were also utilized to characterize the pH-responsive oil-adhesion. The adhesive forces between PAA-G and other oils such as hexane (18.0 mNm^{-1}), chloroform (28.9 mNm^{-1}), tetrachloroethane (33.9 mNm^{-1}) and dichlorobenzene (36.7 mNm^{-1}) are presented in the ESI,† Table S1. The comparison results show that all adhesive forces dramatically decrease when pH value is greater than the PAA pK_a of 4.7. The OCAs of all oils with different surface tensions on PAA-G in the solutions with pH values from 1.0 to 12.0 are listed in Table S2.†

To investigate the reversibility of the pH-responsive oil-adhesion switch, we alternately tested the adhesive force of PAA-G in solutions with pH values of 2.4 and 8.0. The PAA-G was firstly placed in a solution with pH value of 2.4 and the adhesive force was measured. Then, the PAA-G was removed from solution with a pH value of 2.4, rinsed with deionized water and dried by nitrogen. After that, the PAA-G was immersed into a solution with a pH value of 8.0 and measured again. The measurements of adhesive force from 10 consecutive cycles (Fig. 4b) show a good reversibility of this switchable PAA-G surface between high and low oil-adhesion responsive to pH alternation.

We attempted to understand this interesting switching property of oil-adhesion and underwater superoleophobicity on the as-prepared PAA-G surface.[1,2] On this nanostructured rough surface by plasma polymerization, the molecular stimuli-response of PAA plays a key role in obtaining the pH-responsive switchable oil-adhesion surface. The molecular conformation of PAA depends on the degree of dissociation or protonation as a weak polyelectrolyte that is controlled by the pH and ionic strength of the surrounding solution. To further investigate the mechanism of the aforementioned results, we characterized the change in surface morphology of PAA-G in solution with pH values of 4.0 and 5.0 through the underwater AFM, as shown in Fig. 5a and 5b, and the blue dash rectangle in Fig. 5a and 5b shows the mark in the *in situ* processing of underwater AFM testing. The surface morphology of PAA-G changes rough to smooth with pH values increasing from 4.0 to 5.0. When the pH value is below PAA's pK_a of 4.7, the intramolecular hydrogen bonds were formed among the carboxylic acid groups on neighboring PAA branched chains, which leads to a dehydrated coiled state and offers a rough surface and a lower ratio of water content. As a result, the surface shows an OCA below 150° and high adhesion to oil droplets. It is a typical Wenzel state (Fig. 5c) where an oil droplet is in contact with the PAA-G substrate, resulting in high oil-adhesion. On the other hand, when the pH value increases over PAA's pK_a of 4.7, the carboxylic acid groups on the PAA branched chain form intermolecular hydrogen bonds with the surrounding water molecules, which leads to

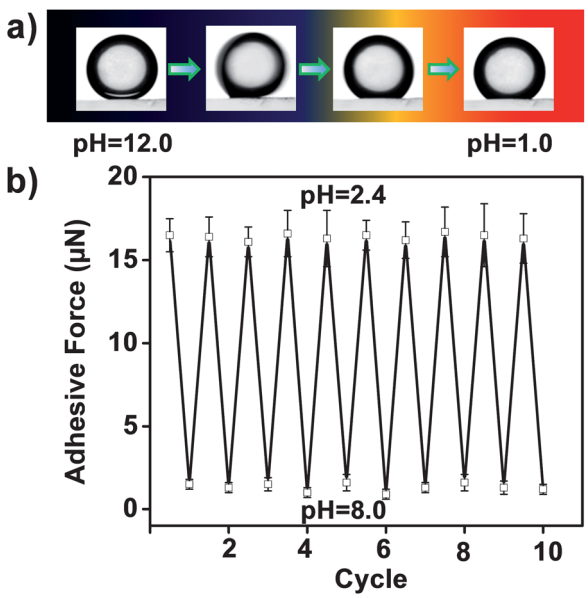

Fig. 4 Reversible pH-responsive switch of oil-adhesion on the PAA-G surface. (a) The *in situ* process of an oil droplet on PAA-G changes from low to high adhesive force by quickly changing the environmental pH value from 12.0 to 1.0. The photographs represent the different adhesion situation with the time sequence in this process. More details are shown in the ESI,† Movie S1. (b) The adhesive force decreases from 16.7 ± 2.1 μN to 1.5 ± 0.4 μN when pH increases from 2.4 to 8.0. The adhesive force can easily switch for 10 cycle times between a pH value of 2.4 and pH value of 8.0, indicating a good reversibility.

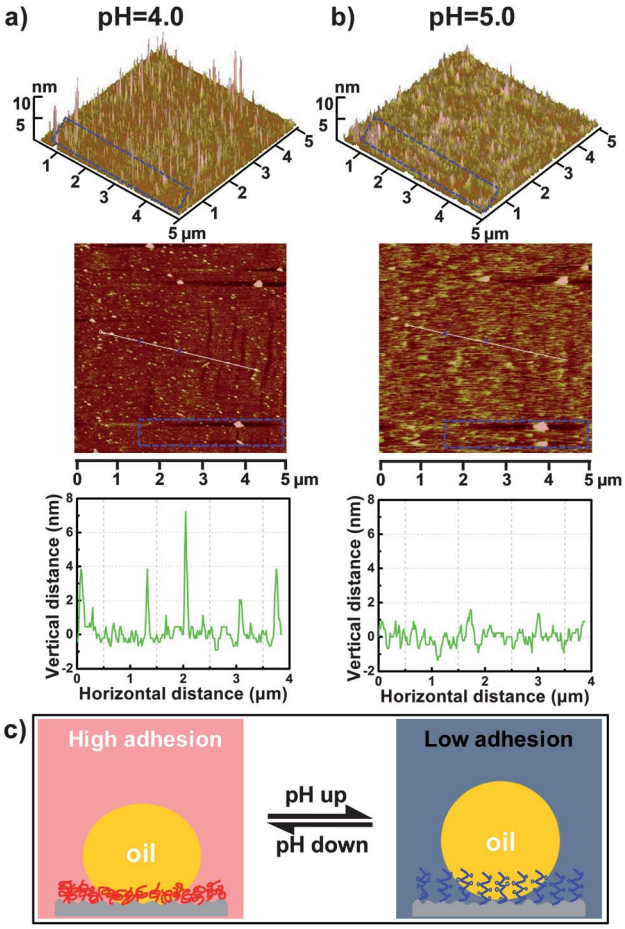

Fig. 5 (a) The underwater AFM image of PAA-G in solution with a pH value of 4.0 shows rough morphology with a roughness of about 4.5 nm. (b) When the pH value increases to 5.0, the surface morphology becomes smooth with a roughness of about 1.5 nm. The blue dash rectangle in Fig. 5a and 5b shows the mark in the *in situ* processing of underwater AFM testing. (c) The proposed mechanism for underwater pH-responsive switchable oil-adhesion. At a low pH, the carboxylic groups on neighboring PAA branched chains form intramolecular hydrogen bonding, which leads to a dehydrated coiled state and thus offers a rough surface and a lower ratio of water content. The oil wetting state is typical of a Wenzel state. However, as for high pH, the carboxylic groups on the PAA branched chain form intermolecular hydrogen bonds with surrounding water molecules, which leads to a hydrated stretched state and thus provides a surface with low roughness and a high ratio of water content. The wetting state changes into a typical Cassie state.

a hydrated stretched state and thus provides the surface with low roughness and high ratio of water content. Thus the wetting state changes into a typical Cassie state (Fig. 5c) with an OCA higher than 150° and low adhesion to oil droplets.

Conclusions

In summary, a smart underwater superoleophobic surface with switchable oil-adhesion was successfully fabricated. This smart surface can reversibly switch between high oil-adhesion at low pH and low oil-adhesion at high pH underwater along with the pH-responsive transition of molecular conformation of PAA. We believe it supplies a promising platform for tuning surface properties and has potential applications in smart microfluidics, controllable bio-adhesion and intelligent materials for oil-removal treatment and marine antifouling

Acknowledgements

This work was supported by the National Research Fund for Fundamental Key Projects (2012CB933800, 2010CB934700, 2009CB930404), the National Natural Science Foundation of China (21175140, 51103004, 21003132, 91127038), the Research Fund for the Doctoral Program of Higher Education (20101102120044 and 20101102110035), the Fundamental Research Funds for the Central Universities (YWF-12-LXGY-017), and the Scientific Research Foundation for the Returned Overseas Chinese Scholars, State Education Ministry, P.R. China.

Notes and references

1 M. J. Liu, S. T. Wang, Z. X. Wei, Y. L. Song and L. Jiang, *Adv. Mater.*, 2009, **21**, 665.
2 Q. Cheng, M. Li, Y. Zheng, B. Su, S. Wang and L. Jiang, *Soft Matter*, 2011, **7**, 5948.
3 M. J. Liu, Y. M. Zheng, J. Zhai and L. Jiang, *Acc. Chem. Res.*, 2010, **43**, 368.
4 Z. Xue, S. Wang, L. Lin, L. Chen, M. Liu, L. Feng and L. Jiang, *Adv. Mater.*, 2011, **23**, 4270.
5 L. Chen, M. J. Liu, H. Bai, P. P. Chen, F. Xia, D. Han and L. Jiang, *J. Am. Chem. Soc.*, 2009, **131**, 10467.
6 F. L. Geyer, E. Ueda, U. Liebel, N. Grau and P. A. Levkin, *Angew. Chem., Int. Ed.*, 2011, **50**, 8424.
7 B. Zhao, J. S. Moore and D. J. Beebe, *Science*, 2001, **291**, 1023.
8 R. Sheparovych, M. Motornov and S. Minko, *Adv. Mater.*, 2009, **21**, 1840.
9 Y. Huang, M. Liu, J. Wang, J. Zhou, L. Wang, Y. Song and L. Jiang, *Adv. Funct. Mater.*, 2011, **21**, 4436.
10 L. Chen, M. J. Liu, L. Lin, T. Zhang, J. Ma, Y. L. Song and L. Jiang, *Soft Matter*, 2010, **6**, 2708.
11 (*a*) M. A. C. Stuart, W. T. S. Huck, J. Genzer, M. Muller, C. Ober, M. Stamm, G. B. Sukhorukov, I. Szleifer, V. V. Tsukruk, M. Urban, F. Winnik, S. Zauscher, I. Luzinov and S. Minko, *Nat. Mater.*, 2010, **9**, 101; (*b*) F. Zhou and W. T. S. Huck, *Phys. Chem. Chem. Phys.*, 2006, **8**, 3815; (*c*) J. F. Mano, *Adv. Eng. Mater.*, 2008, **10**, 515; (*d*) T. Chen, R. Ferris, J. Zhang, R. Ducker and S. Zauscher, *Prog. Polym. Sci.*, 2010, **35**, 94; (*e*) T. Sun and G. Qing, *Adv. Mater.*, 2011, **23**, H57.
12 R. Langer, J. Lahann, S. Mitragotri, T. N. Tran, H. Kaido, J. Sundaram, I. S. Choi, S. Hoffer and G. A. Somorjai, *Science*, 2003, **299**, 371.
13 S. Wang, H. Liu, D. Liu, X. Ma, X. Fang and L. Jiang, *Angew. Chem., Int. Ed.*, 2007, **46**, 3915.
14 T. Sun, G. Wang, L. Feng, B. Liu, Y. Ma, L. Jiang and D. Zhu, *Angew. Chem., Int. Ed.*, 2004, **43**, 357.
15 (*a*) X. Yu, Z. Q. Wang, Y. G. Jiang, F. Shi and X. Zhang, *Adv. Mater.*, 2005, **17**, 1289; (*b*) L. D. Zarzar, P. Kim and J. Aizenberg, *Adv. Mater.*, 2011, **23**, 1442.
16 E. S. Gil and S. M. Hudson, *Prog.Polym. Sci.*, 2004, **29**, 1173.
17 H. Aizawa, S. Kurosawa, K. Kobayashi, K. Kashima, T. Hirokawa, Y. Yoshimi, M. Yoshimoto, T. Hirotsu, J. Miyake and H. Tanaka, *Mater. Sci. Eng., C*, 2000, **12**, 49.
18 (*a*) S. T. Wang, H. Liu and L. Jiang, *Annu. Rev. Nano Res.*, 2006, **1**, 573; (*b*) F. Xia and L. Jiang, *Adv. Mater.*, 2008, **20**, 2842.
19 J. W. Lee, S. Y. Kim, S. S. Kim, Y. M. Lee, K. H. Lee and S. J. Kim, *J. Appl. Polym. Sci.*, 1999, **73**, 113.
20 O. E. Philippova, D. Hourdet, R. Audebert and A. R. Khokhlov, *Macromolecules*, 1997, **30**, 8278.
21 A. K. Bajpai, *Prog. Polym. Sci.*, 1997, **22**, 523.

Addition and correction

View Online

Note from RSC Publishing

This article was originally published with incorrect page numbers. This is the corrected, final version.

The Royal Society of Chemistry apologises for these errors and any consequent inconvenience to authors and readers.